HHS Public Access

Author manuscript

Antiviral Res. Author manuscript; available in PMC 2023 April 30.

Published in final edited form as:

Antiviral Res. 2022 December ; 208: 105457. doi:10.1016/j.antiviral.2022.105457.

An optimized cell-based assay to assess influenza virus replication by measuring neuraminidase activity and its applications for virological surveillance

Mira C. Patel[a], **Daniel Flanigan**[a,b], **Chenchen Feng**[a,c], **Anton Chesnokov**[a], **Ha T. Nguyen**[a], **Anwar Abd Elal**[a,d], **John Steel**[a], **Rebecca J. Kondor**[a], **David E. Wentworth**[a], **Larisa V. Gubareva**[a,*], **Vasiliy P. Mishin**[a]

[a]Influenza Division, National Center for Immunization and Respiratory Diseases, Centers for Disease Control and Prevention, Atlanta, GA, USA

[b]General Dynamics Information Technology, Atlanta, GA, USA

[c]Oak Ridge Institute for Science and Education, Oak Ridge, TN, USA

[d]Cherokee Nation Integrated Health, L.L.C., Atlanta, GA, USA

Abstract

Year-round virological characterization of circulating epidemic influenza viruses is conducted worldwide to detect the emergence of viruses that may escape pre-existing immunity or acquire resistance to antivirals. High throughput phenotypic assays are needed to complement the sequence-based analysis of circulating viruses and improve pandemic preparedness. The recent entry of a polymerase inhibitor, baloxavir, into the global market further highlighted this need. Here, we optimized a cell-based assay that considerably streamlines antiviral and antigenic testing by replacing lengthy immunostaining and imaging procedures used in current assay with measuring the enzymatic activity of nascent neuraminidase (NA) molecules expressed on the surface of virus-infected cells. For convenience, this new assay was named IRINA (Influenza Replication Inhibition Neuraminidase-based Assay).

IRINA was successfully validated to assess inhibitory activity of baloxavir on virus replication by testing a large set (>150) of influenza A and B viruses, including drug resistant strains and viruses collected during 2017–2022. To test its versatility, IRINA was utilized to evaluate neutralization activity of a broadly reactive human anti-HA monoclonal antibody, FI6, and post-infection ferret antisera, as well as the inhibition of NA enzyme activity by NA inhibitors. Performance of IRINA was tested in parallel using respective conventional assays.

*Corresponding author. 1600 Clifton Road, MS-H17-5, Atlanta, GA, 30329-4027, USA., lgubareva@cdc.gov (L.V. Gubareva).

Declaration of competing interest

The authors declare that they have no known competing financial interests or personal relationships that could have appeared to influence the work reported in this paper.

Appendix A. Supplementary data

Supplementary data to this article can be found online at https://doi.org/10.1016/j.antiviral.2022.105457.

IRINA offers an attractive alternative to current phenotypic assays, while maintaining reproducibility and high throughput capacity. Additionally, the improved turnaround time may prove to be advantageous when conducting time sensitive studies, such as investigating a new virus outbreak. This assay can meet the needs of surveillance laboratories by providing a streamlined and cost-effective approach for virus characterization.

Keywords

Influenza; Neuraminidase; Antiviral resistance; HINT; Baloxavir; NA inhibitor

1. Introduction

Influenza viruses are respiratory pathogens of high consequence to public health as they are responsible for near annual epidemics of various severity and can sporadically cause pandemics. Infection control measures include non-pharmaceutical interventions (masking, social distancing, etc.), vaccination, and use of antivirals. Virological surveillance is carried out year-round to identify influenza viruses in circulation (e.g., types, subtypes) and characterize representative viruses using an array of laboratory methods (Jester et al., 2018). CDC conducts influenza virological surveillance in the United States (US) and participates in the World Health Organization's Global Influenza Surveillance and Response System (WHO GISRS) as one of the seven WHO Collaborating Centers (https://www.cdc.gov/flu/weekly/overview.htm).

In recent years, high throughput sequence-based methods, such as codon-complete gene segment next generation sequencing (NGS), became a primary tool in global influenza surveillance. NGS allows for simultaneous monitoring of virus evolution, gene reassortment, and detecting previously established molecular determinants associated with antigenic drift, antiviral resistance, and other viral properties. Special attention is given to antigenicity of circulating and emerging viruses, their relatedness to vaccines, and susceptibility to antivirals. Seasonal vaccines require frequent updates to their composition, especially the A(H3N2) subtype component. For many years, the hemagglutination inhibition assay has been the gold standard assay for antigenic analysis. However, ability of recent A(H3N2) viruses to agglutinate RBCs has decreased due to changes in their receptor binding characteristics. Thus, hemagglutination inhibition is no longer considered as a reliable method for characterizing A(H3N2) viruses (Lin et al., 2015). Instead, microneutralization assays with various modifications have been employed for antigenic analysis (Gross et al., 2017; Lin et al., 2015; van Baalen et al., 2017). In general, implementing cell-based assays is challenging as they often tend to show less than desirable inter- and intra-assay consistency and this affects their validation and utility. Recently, we developed a single-cycle cell-based assay known as high content imaging-based neutralization test (HINT), in which we introduced several innovative modifications that allowed for greater consistency in testing outcomes (Jorquera et al., 2019). This assay has successfully been used to conduct antigenic analysis (Jorquera et al., 2019; Mohan et al., 2021) and generate surveillance data for the WHO vaccine composition consultations.

Notably, cell-based assays have not been used widely to monitor susceptibilities to older classes of approved influenza antivirals, M2 inhibitors and neuraminidase (NA) inhibitors (NAIs). For M2 inhibitors, markers of resistance are well-established and common for all type A viruses (e.g., M2-S31N), hence susceptibility monitoring has primarily been confined to sequence-based analysis (Deyde et al., 2007). For NAIs, cell-based assays were shown to be unreliable (Gubareva, 2004; Tisdale, 2000). Instead, a surrogate phenotypic test based on the inhibition of NA enzyme activity (NA inhibition, NI) has been used in conjunction with NA sequence analysis. Notably, numerous NA substitutions or deletions and their combinations have been reported to affect susceptibility to one or more NAIs, and this necessitates continuous testing of virus isolates using NI assay (https://cdn.who.int/media/docs/default-source/2021-dha-docs/1.-updated-hum_nai_rsm-table_03.05.22_to-post.pdf).

With the recent approval of the polymerase inhibitor, baloxavir marboxil, the use of cell-based assays for monitoring susceptibility has become a necessity. The active metabolite, baloxavir acid (baloxavir), exerts antiviral activity by binding to the polymerase acidic (PA) subunit of viral RNA polymerase, hindering the cap-dependent endonuclease activity and hence virus replication (Noshi et al., 2018). Both multi-cycle focus reduction assay (FRA) and single-cycle HINT have successfully been used to monitor susceptibility to baloxavir (Govorkova et al., 2022; Gubareva et al., 2019; Takashita et al., 2018). The baloxavir effective concentration yielding 50% reduction in virus replication (EC_{50}) differs between the two assays; however, they have good consistency in fold increase associated with PA amino acid substitutions (Takashita et al., 2020b). This allows for the harmonization of test results for global surveillance purposes (Govorkova et al., 2022; Gubareva et al., 2019). While there is no established threshold for reporting resistance to baloxavir, a provisional threshold for reduced susceptibility has been set at ≥3-fold (Govorkova et al., 2022; Gubareva et al., 2019). Based on the current available data, this threshold is likely to capture >95% of potential baloxavir-resistance conferring mutations (Ince et al., 2020). Moreover, this threshold is successfully being employed by WHO-antiviral working group members in their global update to describe findings on phenotypic susceptibility testing of influenza viruses to baloxavir conducted by the Atlanta and Tokyo WHO Collaborative Centers using HINT and FRA, respectively (Govorkova et al., 2022). Amino acid substitutions at residue 38 of PA protein are considered the primary pathway for the emergence of baloxavir resistance, with the change of isoleucine (I) to threonine (T) being most frequently reported (Hayden et al., 2018; Omoto et al., 2018). Changes at other PA residues (e.g., E23G) have also been detected following baloxavir treatment, albeit at low frequency (Ince et al., 2020). PA substitutions are shown to confer a wide range of fold increases in EC_{50}, and this effect may depend on virus type and subtype (https://cdn.who.int/media/docs/default-source/influenza/summary-of-polymerase-acidic-(pa)-protein-amino-acid-substitutions-analysed-for-their-effects-on-baloxavir-susceptibility.pdf).

Like other assays, HINT consists of two steps: 1) determination of virus working dilution (normalization of virus inoculum), and 2) assessment of virus replication in the presence of either an antiviral (inhibition) or antibody (neutralization, which is commonly assessed after pre-incubation of virus with antibody). Some of the salient improvements HINT introduced were: 1) skipping preparation of a cell monolayer prior to inoculation by adding a cell suspension directly to a well containing virus (or virus-antiviral/antibody mixture),

2) using inoculum at low multiplicity of infection (~0.03), 3) limiting virus replication to a single-cycle by omitting trypsin from virus growth media, thereby minimizing inconsistency due to varying replicative rates of different viruses, and 4) employing specialized imaging platforms (automated microplate digital microscopy) for improved accuracy in counting virus-infected cells (Gubareva et al., 2019; Jorquera et al., 2019). However, certain procedures that are required at both steps of HINT (e.g., immunostaining with primary anti-nucleoprotein (NP) antibody followed by incubation with secondary antibody and DNA dye) are laborious and time consuming. This cumbersome procedure and the need for specialized equipment lengthens the assay turnaround time and hinders prospects for wider implementation.

In this study, we aimed to find solutions to overcome these limitations of HINT, while preserving its utility, consistency, and other valuable attributes. Measurement of NA enzyme activity as an indicator of virus replication in cell culture has previously been recognized as an appealing approach (Eichelberger et al., 2008; Hassantoufighi et al., 2010; Jorquera et al., 2019; Lin et al., 2017; Nayak and Reichl, 2004). In an earlier study, NA activity was used during development of a downstream process for the purification of equine influenza virus in vaccine manufacturing (Nayak and Reichl, 2004). Our laboratory, as well as others, routinely measure the NA activity in cell culture supernatants to determine when to harvest virus isolates for characterization (Jorquera et al., 2019; Lin et al., 2017). Furthermore, a virus neutralization assay that used NA activity to quantify influenza replication was developed (accelerated viral inhibition assay with NA as readout – AVINA assay). Its usefulness was demonstrated for high throughput screening of antivirals with different mechanisms of action and quantifying HA and NA-inhibiting antibody responses (Eichelberger et al., 2008; Hassantoufighi et al., 2010). However, we were unable to find published reports indicating that this assay can meet requirements of virological surveillance.

Consequently, we explored whether consistent testing outcomes delivered by HINT can be maintained when immunostaining and cell counting are replaced by measuring NA activity. In this study, we determined experimental conditions that allow for using enzyme activity of nascent NA molecules expressed on the surface of virus-infected cells as a reliable and consistent indicator of virus replication. For convenience, the new assay was named IRINA (*I*nfluenza *R*eplication *I*nhibition *N*euraminidase-based *A*ssay) to distinguish it from the conventional HINT. We also demonstrated that IRINA has a potential to improve virological surveillance by providing a streamlined unifying approach for comprehensive antiviral and antigenic testing.

2. Materials and methods

2.1. Viruses

Influenza viruses used in this study were submitted to the WHO Collaborating Center for Surveillance, Epidemiology and Control of Influenza at the CDC by US public health laboratories (PHLs) and other laboratories participating in WHO-GISRS.

Most A(H1N1)pdm09 and type B viruses were propagated in MDCK cells, whereas A(H3N2) and a few A(H1N1)pdm09 (from 2021) viruses were propagated in MDCK-SIAT1 cells (Matrosovich et al., 2003). A set of 96 epidemic viruses, representing two A subtypes and two B lineages (n = 24 for each subtype and lineage), collected during 2017–2021 was used in this study. These viruses were selected to represent the diverse genetic groups of viruses in circulation. In addition, a separate set of A (H3N2) viruses (n = 53) collected in the US during the 2021–2022 season was tested as specified in Results.

CDC antiviral susceptibility reference virus panels (International Reagent Resource (IRR); FR-1678 and FR-1755) and other viruses displaying reduced susceptibility to baloxavir and NAIs were also tested (Supplementary methods).

2.2. Neuraminidase substrate

NA activity was measured using a conventional NA assay, whereby the cleavage of substrate 2-(4-(methylumbelliferyl)-a-D-N-acetylneuraminic acid (MUNANA) results in the release of the fluorescent product 4-methylumbelliferone (4-MU). NA substrate from NA-Fluor™ Influenza Neuraminidase Assay Kit (Applied Biosystems) was used to prepare a 200 μM working solution in assay buffer (alternatively, 200 μM MUNANA (Sigma Aldrich) in 33.3 mM MES buffer, 4 mM $CaCl_2$, pH 6.5). A 4-MU (Sigma Aldrich) calibration curve (100–3200 pmol) was used to establish the relationship between target NA activity of reference viruses and pmol of 4-MU.

2.3. Influenza replication inhibition neuraminidase-based assay (IRINA)

For the initial step of virus titration (inoculum normalization), the test viruses were serially diluted in a 96-well microplate (black clear-bottom plate, Agilent) from 10^{-1} to 10^{-7} in virus growth medium (VGM; DMEM supplemented with 0.2% bovine serum albumin, 25 mM HEPES, 100 U/mL penicillin, 100 μg/mL streptomycin) without TPCK-trypsin to achieve single-cycle virus replication as described for HINT (Supplementary methods, Fig. S1 IRINA workflow). After adding a 50 μL single-cell suspension of MDCK-SIAT1 into wells (0.3×10^5 cells/well) containing 100 μL diluted virus, the microplates were incubated at 37 °C in 5% CO_2 for 24 h. Supernatants were then aspirated and 50 μL of NA substrate (200 μM) was added on top of the infected cell monolayer followed by incubation at 37 °C in 5% CO_2 for 1 h. The reaction was stopped by adding 50 μL of NA-Fluor™ stop solution (alternatively, 0.2 M Na_2CO_3, pH 11.5) to each well and fluorescence measured from the bottom surface of plates using Cytation 7 (BioTek) with an excitation filter (λ = 360 nm) and an emission filter (λ = 460 nm). The NA activity-based virus dilution yielding fluorescence signal equivalent to ~1750 or ~900 pmol/well of 4-MU for type A and type B viruses, respectively (rationale for this is described below in Results section 3.1), was determined and used in the next inhibition step (Fig. S1).

For inhibition by baloxavir, 3-fold serially diluted baloxavir at 3X in VGM without TPCK-trypsin (~0.02–333 nM; with a final concentration of ~0.006–111 nM) was used. 50 μL of each baloxavir dilution was mixed with 50 μL of diluted virus (based on NA activity as described above) in a 96-well microplate, followed by addition of 50 μL of cell suspension without pre-incubating virus-baloxavir mixture. Plates were incubated at 37 °C in 5% CO_2

for 24 h followed by determination of NA activity of infected cells as described above for titration step. To test neutralization by monoclonal antibody (mAb) or ferret antisera raised against cell-propagated vaccine reference viruses, 2-fold serially diluted mAb at 2X (0.16–20 μg/mL; final concentration of 0.08–10 μg/mL) or antiserum (starting at 1/40; final starting dilution of 1/80), both diluted in VGM without TPCK-trypsin, was mixed 1:1 with diluted virus and incubated for 1 h at RT prior to the addition of cells. The rest of the steps were same as described for baloxavir (Fig. S1).

After inhibition, the relative fluorescence unit (RFU) readouts were curve-fitted using nonlinear regression to determine EC_{50} values or neutralization titers as previously described (Okomo-Adhiambo et al., 2013; Jorquera et al., 2019).

2.4. NI assay and IRINA to assess susceptibility to NAIs

NI assay was carried out as previously described (Okomo-Adhiambo et al., 2013). To assess susceptibility to NAIs using IRINA, the initial set-up was identical as described above for baloxavir, but in the absence of any antiviral (Fig. S1). Following 24 hpi, supernatants were aspirated; 50 μL of serially 2X half-log_{10} diluted NAIs (0.06–2000 nM) were added to corresponding wells with infected cell monolayers and plates were incubated for 1 h at 37 °C in 5% CO_2. Next, 50 μL of NA substrate (200 μM) was added to each well (final NAI concentration 0.03–1000 nM) followed by incubating plates at 37 °C in 5% CO_2 for 1 h. The reaction was stopped by adding 100 μL of stop solution to each well and fluorescence was measured as described above.

Determination of drug concentration required to inhibit NA activity by 50% (IC_{50}) was carried out as described above (Okomo-Adhiambo et al., 2013). Fold changes in IC_{50} were determined by comparing the IC_{50} values of test viruses with those of the NA sequence-matched control viruses and were interpreted according to WHO classification criteria (WHO 2012).

3. Results

3.1. Normalization of virus inoculum based on NA activity

We hypothesized that HINT can be streamlined if the immuno-staining and digital microscopy utilized to count virus-infected cells are replaced with the NA activity measurement. To achieve this, we needed to demonstrate that: 1) NA protein synthesized under HINT experimental conditions has sufficient enzyme activity for a conventional fluorescent NA assay, and 2) there is a direct correlation between the number of infected cells and NA activity.

One of the key requirements of HINT is the normalization of virus inoculum to produce 1000 infected cell population (ICP); acceptable range 300–4000. To this end, three influenza viruses, A(H1N1)pdm09, A (H3N2), and B/Victoria, were serially diluted in microplates and cell suspension was added. At 24 hpi, ICP values were determined using HINT while NA activity was measured in parallel plates using NA assay. Initially, NA activity was measured separately in the harvested cell culture supernatants and the cell monolayers. Although NA activity was detected in supernatants, the fluorescent signal was low and inconsistent, which

would be expected under conditions of a single-cycle virus replication (Fig. S2). Conversely, the NA activity of nascent (budding) NA molecules on the surface of infected cells was much greater than in supernatants (Fig. S2). As evident from Fig. 1, NA activity (expressed in RFU) was also in a linear range, especially when the respective ICP values were within the acceptable range. Specifically, a strong correlation (r = 0.977–0.992) was observed between 300 and 4000 ICP and corresponding RFU values for all three viruses. Noteworthy, the RFU and ICP for the B/Victoria virus maintained a linear relationship up to the highest tested 6000 ICP (Fig. 1).

These results supported our hypothesis, however, we wanted to ascertain how to calculate proper virus inoculum without relying on immunostaining and cell imaging. We argued that by targeting a specific fluorescent signal corresponding to ~1000 ICP, we could normalize virus inoculum based on NA activity. To determine this target signal, we first assessed the consistency of NA activity of the same three viruses diluted to yield ~1000 ICP. In a series of independent experiments, we determined the average ICP values (total of 81–149 replicates), which showed good consistency: 1158 ± 210, 1138 ± 314, and 1330 ± 364, for A(H1N1)pdm09, A(H3N2), and B/Victoria, respectively (Table 1). Notably, the respective NA activity readings were also reasonably consistent, 27189 ± 5986, 28384 ± 6181, and 15805 ± 6398. The target NA activity was similar for the two influenza A viruses and was ~2-fold lower for the type B virus. Additionally, we found that the NA activity corresponding to ~1000 ICP for a B/Yamagata virus was comparable to that of a B/Victoria virus (Table S1). The ~2-fold lower target NA activity for type B viruses is not surprising because the temperature used for virus replication was 37 °C, which is suboptimal for type B viruses. Moreover, replication cycle of type B viruses is considered to be longer than type A viruses (Karakus et al., 2018).

The target NA activity determined for a reference virus can be used to calculate a working dilution of a test virus of the same type. However, this approach has downsides for a broader assay implementation (reference virus stock maintenance, stock variability, etc.). In addition, absolute RFU values differ depending on the fluorimeter used. Therefore, we explored whether it would be possible to use the fluorescent metabolite 4-MU for this purpose. 4-MU was serially diluted to generate a calibration curve to establish a correlation between 4-MU concentrations and RFU values (Fig. S3). Using the respective linear curve equation, the median target NA activities shown in Table 1 were converted into 4-MU concentrations: 1755, 1759, and 909 pmol for A(H1N1) pdm09, A(H3N2), and B viruses, respectively. Using this approach, type A and type B viruses could be diluted to yield a fluorescent NA activity signal that is produced by ~1750 and ~900 pmol/well of 4-MU, respectively. This NA activity would then correspond to ~1000 ICP.

In the next experiment, we tested this approach using a set of 96 influenza A and B viruses. For each virus, two dilution factors were calculated based on NA activity (IRINA) and ICP (HINT). For each individual virus, the two dilution factors were comparable; the average ratios (IRINA dilution factor/HINT dilution factor = ratios of dilution factors) for each group of viruses were 1.0 ± 0.3, 0.8 ± 0.2, 1.1 ± 0.3, and 1.2 ± 0.3 for A(H1N1)pdm09, A(H3N2), B/Victoria, and B/Yamagata viruses, respectively (Table S2). These viruses were diluted according to their NA activity-based dilution factor and the actual ICP values were

determined. Indeed, the ICP values for these viruses fell within the acceptable ICP range (data not shown). A single exception in this set of viruses was the A(H3N2) virus, A/Illinois/10/2020, which displayed a low ratio (1625:14481 = 0.1) (Table S2). This result was indicative of uncharacteristically low NA activity. Interestingly, the NA of this virus has a rare amino acid substitution N419S (EPI1740465; one out of ~29000 A(H3N2) NA sequences since 2018), which may affect NA activity or stability. Expectedly, the ICP produced by this virus when diluted according to its NA activity was too high (~6000) and out of the acceptable range (data not shown).

Taken together, these results support our hypothesis that for most epidemic influenza viruses, measuring enzyme activity of cell-associated nascent NA protein may offer a feasible alternative to immunostaining of NP protein to achieve normalization of virus inoculum. Next, we wanted to test whether this approach could be used to reliably assess inhibition of virus replication.

3.2. Susceptibility to polymerase inhibitor baloxavir

In the next series of experiments, we evaluated whether IRINA is suitable for monitoring susceptibility to baloxavir. First, we wanted to know whether IRINA-generated baloxavir EC_{50} values would remain consistent when viruses are tested using varying inoculum. The same three viruses were diluted to give a range of NA activity corresponding to 300–4000 ICP and inhibition with baloxavir was carried out (Fig. S4). For both influenza A viruses, the IRINA EC_{50}s remained consistent (<2-fold difference in EC_{50}) when their NA activity was ~8000–40000 RFU, corresponding to 300–3000 ICP (Fig. S4). However, EC_{50} was slightly elevated (~2.5-fold) when NA activity was >50000 RFU. For the influenza B virus, the IRINA EC_{50}s were consistent across the entire tested range (Fig. S4).

It is known that baloxavir EC_{50} values often differ depending on virus (sub)type and method used (e.g., FRA vs HINT). Therefore, baloxavir susceptibility monitoring relies on the ability of an assay to detect viruses displaying reduced susceptibility, which is defined as a ≥ 3-fold increase in EC_{50} compared to either a control virus or a (sub)type-specific median EC_{50}. At CDC, two A(H3N2) reference viruses, A/Louisiana/50/2017-PA-I38 (wildtype) and A/Louisiana/49/2017-PA-I38M (reduced susceptibility) are routinely used in each HINT-based baloxavir susceptibility test for quality control purposes. This pair of reference viruses was tested multiple times using IRINA and HINT to evaluate the consistency of EC_{50}s and corresponding fold increases. In IRINA, the median EC_{50}s of PA-I38 and PA-I38M-substituted viruses were 1.13 and 17.42 nM, respectively; corresponding fold increase in EC_{50} was 15 (Fig. 2A). In HINT, the median EC_{50}s of these viruses were 1.10 and 12.18 nM, respectively, which corresponded to an 11-fold increase (Fig. 2A). The median EC_{50} of PA-I38 virus was similar ($P > 0.05$) between both methods, while median EC_{50} of PA-I38M-substituted virus varied ($P < 0.05$). Despite this variation in EC_{50} values, fold increases determined using IRINA and HINT were consistent (within < 2-fold), thus supporting the suitability of IRINA.

Next, we extended the reduced susceptibility analysis to a larger set of viruses carrying various PA amino acid substitutions (Table 2). HINT EC_{50} and fold increase values for these viruses were available from previous tests and used to compare results obtained using

IRINA. The fold increases in EC_{50}s conferred by all tested PA substitutions were similar (< 2 times different) between the two assays (Table 2). Notably, we were able to detect mild increases (3–10-fold) in EC_{50} conferred by various PA substitutions (e.g., E23G) using IRINA. Moreover, for PA substitutions (e.g., L28P) that conferred < 3-fold increase in HINT, the outcome of the IRINA testing was the same (Table 2).

IRINA was also applied to determine baloxavir EC_{50} values for the set of surveillance viruses (n = 96) used above (Table S2). These viruses did not contain any PA amino acid substitutions of concern. All viruses had EC_{50} values below the 3-fold threshold, which was consistent with HINT data (Fig. 2B and 2C). Median EC_{50}s determined by both assays were highly comparable ($P > 0.05$) for both A subtypes and B/Yamagata lineage viruses, while medians were found to be significantly different for B/Victoria lineage viruses ($P < 0.05$). Of note, for A/Illinois/10/2020 (H3N2), which has uncharacteristically low NA activity, displayed similar EC_{50}s in HINT (1.3 nM) and IRINA (1.4 nM), despite having been diluted to an out-of-range ICP in the latter assay. This result indicates the robustness of NA activity-based measurement and suggests that IRINA can be used for testing viruses with inherently low NA activity. Taken together, these data strongly support the suitability of IRINA to conduct baloxavir susceptibility monitoring.

3.3. Susceptibility to a broadly neutralizing anti-HA monoclonal antibody

Neutralization assays are commonly applied to assess the antiviral activity of HA-targeting mAbs, some of which have reached clinical trial stage of development (Kallewaard et al., 2016). Here, we assessed the neutralization activity of the human mAb FI6 against the A(H3N2) viruses (n = 24) using both IRINA and HINT (Corti et al., 2011). HAs of the tested viruses belong to antigenically distinct subclades 3C.3a and 3C.2a. The procedure was the same as that for baloxavir testing, except diluted viruses were pre-incubated with mAb prior to adding cell suspension. All tested viruses were neutralized by this mAb. The median EC_{50} values determined by IRINA and HINT assays were comparable (1.77 vs. 1.15, respectively; not statistically different $P > 0.05$) with ranges of 0.28–5.34 and 0.26–5.48 μg/mL, respectively (Fig. S5).

3.4. Application of IRINA for assessing susceptibility to NAIs

Although cell-based assays are not recommended for assessing susceptibility to NAIs (Tisdale, 2000), we wanted to see if the IRINA could be used. We argued that it is plausible if we only utilize the nascent NA molecules on the infected cells as the source of NA activity to set up a biochemical reaction to test inhibition. Moreover, we showed above that in IRINA the normalized virus inoculum generates consistent NA activity signal, which falls in a linear range, as required for the conventional NI assay.

To this end, IRINA was modified to determine IC_{50} values for oseltamivir, zanamivir, peramivir, and laninamivir. For this experiment, we used NA mutants and their wildtype counterparts from the CDC NAI susceptibility reference panel and other type A and B viruses that carry various NA amino acid substitutions known to reduce susceptibility. Some of these substitutions are also known to reduce NA activity (e.g., N2-R292K). NI IC_{50} values for these viruses were available from previous tests and used to compare results

obtained using IRINA (Table 3, virus dilutions used for both assays are provided in Table S3).

Although both assays utilize the same substrate (NA-Fluor™) and were essentially carried out under the same conditions, IRINA IC_{50}s were ~1.5î.6 times higher than those obtained using the NI assay (Table 3). This is likely to be attributed to the difference in the source of the NA activity; NA expressed on the infected cells vs virus in suspension. Importantly, reduced (highly) inhibition (RI/HRI) to one or more NAIs conferred by NA substitutions were similar between these two assays (Table 3), which is the most relevant metric for antiviral surveillance (WHO 2012). Minor disagreements were observed when interpreting the fold increases for the viruses displaying borderline values (Table 3).

3.5. Antiviral and antigenic analysis of A(H3N2) viruses, 2021-2022

The beginning of the northern hemisphere 2021–2022 season in the US was marked by large outbreaks caused by A(H3N2) viruses. This provided an attractive opportunity to use IRINA for simultaneous antiviral and antigenic analysis. A set of A(H3N2) viruses (n = 53) was tested in parallel against the four FDA-approved antivirals. All A(H3N2) viruses were susceptible to baloxavir with mean EC_{50} values 0.91 ± 0.21, which was similar to the subtype-specific median of 1.19 nM determined using HINT during 2019–2020 (n = 82). Similarly, all viruses were susceptible to oseltamivir, zanamivir, and peramivir with mean IRINA IC_{50} values of 0.32 ± 0.07, 0.53 ± 0.10, and 0.24 ± 0.06 nM, respectively.

Phylogenetic analysis of the HA genes of these A(H3N2) viruses showed that all viruses belonged to genetic clade 3C.2a1b.2a.2. To screen viruses for antigenic differences, 18 representative viruses, with HA amino acid differences, were chosen and tested by IRINA and HINT (Table 4). Two viruses representing recent vaccines and their respective homologous post-infection ferret antisera were included in the test. In IRINA, antiserum raised against cell-propagated A/Cambodia/e0826360/2020 showed reduced reactivity (4.9–22.7-fold) with all tested viruses. Conversely, antiserum raised against cell-propagated A/Darwin/6/2021, which belongs to the same HA clade as the tested viruses, reacted well with most of them. Notably, the reactivity of this antiserum was reduced by 2.9î.1-fold (IRINA) and by 3.2–4.7-fold (HINT) if viruses contained either an amino acid change R222K or a combination of S205F + A212T in HA (Table 4). Therefore, antigenic analysis performed using IRINA and HINT showed similar results.

4. Discussion

Development and implementation of high throughput assays for phenotypic characterization is essential for global influenza virological surveillance. Although HINT has proven to be useful and robust, its implementation is limited to laboratories equipped with specialized imaging platforms. Here, we developed a new assay, IRINA, and showed its utility for comprehensive antiviral and antigenic analysis. In the development of IRINA, we preserved many technical solutions that contributed to the success of HINT, while replacing the cumbersome immunostaining and imaging with much simpler and faster NA activity measurement. These advancements were achieved without an apparent loss in the testing outcome, consistency, and reproducibility.

The principle of NA activity as a readout of virus replication has previously been utilized to develop the virus neutralization-AVINA assay (Eichelberger et al., 2008; Hassantoufighi et al., 2010). AVINA depends on multi-cycle replication of virus in the presence of trypsin followed by NA activity measurement either in supernatant or infected cells at 20 hpi. Multi-cycle replication for such a short period of time could be unpredictable due to varying replication kinetics of different influenza viruses. Assay sensitivity was shown to depend on the infectious dose added to the wells. The appropriate virus inoculum for AVINA needs to yield a signal of (1–2) x 10^5 RFU after 20 hpi, indicating a very narrow range (2-fold) for the target NA activity (Hassantoufighi et al., 2010). It is not uncommon to see a half $\log_{10}$ (~3-fold) variation in titer during virus titration, which may depend on virus preparation, cell culture condition, or both (Ruppach, 2013). Phenotypic assays often require optimization to deliver consistent results when testing viruses that may possess different receptor-binding preferences, replication kinetics, or trypsin dependency for multi-cycle replication. Though this approach appeared to be attractive, its utility for surveillance purposes appears to be limited.

Conversely, with single-cycle replication, we demonstrate a strong linear relationship between ICP (range of 300–000) and NA activity of infected cells. This wider range of inoculum accommodates the usual half $\log_{10}$ (~3-fold) variation in titration. We believe that the consistency of IRINA's output strongly relies on the accurate virus titration based on NA activity. By testing (sub)type-specific reference viruses multiple times, we identified the target NA activity, which should be achieved to yield consistent infection and reproducible results for test viruses. To accommodate for different fluorimeters that may be used to detect fluorescence, we correlated the type-specific target NA activity to the fluorescent metabolite, 4-MU concentration. This information would aid laboratories in their normalization of virus inoculum. Using this approach, we demonstrated that dilution factors calculated based on NA activity and ICP were comparable for a large set of surveillance viruses. Concordantly, dilution of viruses based on their NA activity gave corresponding ICP within the acceptable range, indicating robustness of this approach.

This study demonstrates the utility of IRINA for the assessment of susceptibility to antivirals with different mechanisms of action (baloxavir, anti-HA mAb, and NAIs). Moreover, we assessed antigenic relatedness of circulating A(H3N2) viruses to the candidate vaccine viruses. The application of IRINA would unify and streamline different laboratory tests, since several steps, such as cell preparation, virus inoculum, infection time and read out, etc., are the same whether testing against antivirals or antisera (Fig. S1 IRINA workflow).

WHO-GISRS laboratories in countries where baloxavir has recently been approved would benefit from implementing assays for susceptibility monitoring. Two cell-based assays, FRA and HINT, were validated for this purpose (Govorkova et al., 2022). Like HINT, FRA also relies on immunostaining and sophisticated equipment (Takashita et al., 2018). Conversely, IRINA requires a plate fluorimeter that many laboratories have or can obtain more readily. This reduced dependence on specialized instrumentation could make IRINA's implementation more feasible. We observed subtle differences in baloxavir EC_{50} values between IRINA and HINT, however, fold increases in EC_{50} of mutant viruses compared to control viruses were in good agreement. The approach of comparing fold increase in

EC_{50} has been used previously to harmonize NAI and baloxavir susceptibility testing and reporting by WHO GISRS (Govorkova et al., 2022; Meijer et al., 2014). Notably, IRINA also demonstrates that some previously reported markers (e.g., PA-L28P and PA-I38V) had no effect on baloxavir phenotype, which is consistent with previous HINT results when compared to sequence-matched control viruses (Govorkova et al., 2022; Gubareva et al., 2019).

Moreover, IRINA can be used to assess virus susceptibility to NAIs. Although, differences in absolute IC_{50} values between IRINA and NI assay were observed, the interpretation of IC_{50} fold increases were similar. Clinical specimens or virus isolates often contain mixed populations of NA variant and wildtype viruses. In this study, we did not test such virus isolates using IRINA. As IRINA is a single-cycle replication-based assay, where virus is infecting cells without any selection pressure, there is no chance for wildtype or variant viruses to outcompete with each other and change in percentages of their respective populations. Therefore, we do not expect much change in results of IRINA vs. NI assay while testing such isolates. IRINA may provide some advantages, as it requires a smaller quantity of virus (Table S3), which may save time and resources needed for preparing virus isolates and determining a virus working dilution. Additionally, it is known that some NA mutants may have difficulty egressing from the cell surface due to lower NA activity (Barman et al., 2004), but this is not critical when applying IRINA as the source of the enzyme activity are cell-bound NA molecules.

Eichelberger and colleagues have suggested that since NA is the readout of AVINA assay, viruses deficient in NA activity could not be tested (Eichelberger et al., 2008). Using IRINA, we could test many NA mutants (e.g., NA-R292K) that are known to have low NA activity. For example, A(H3N2) virus containing NA-N419S, which has very low NA activity, displayed similar baloxavir EC_{50} in HINT and IRINA, although it required a higher virus inoculum in IRINA. One can argue that an NA activity-based dilution for viruses with inherently low NA activity may result in ICP that is out-of-range. However, we and others noted that compared to NP immunostaining, the range of linearity (quantitative range) is wider for assays that use NA activity as a readout, and this contributes to the robustness of IRINA (Hassantoufighi et al., 2010). Therefore, we believe that testing viruses with low NA activity should not present a significant problem for IRINA.

As with other cell-based assays, the success of IRINA testing depends on availability and proper maintenance of cell cultures, including attention to passage requirements and accurate cell counting for plating. Cell lines may share the same name (e.g., MDCK), but they often exhibit different morphology and other properties due to difference in passage histories and other conditions. It is important to keep in mind that some A(H1N1)pdm09 and other viruses have occasionally been seen to produce a multi-cycle infection in MDCK cell lines. Therefore, to ensure a single-cycle replication, it is best to use a well characterized cloned version of MDCK cell line, like SIAT1 (Matrosovich et al., 2003) or hCK (Takada et al., 2019) or to confirm a lack of multi-cycle replication in the available cell line in the absence of trypsin. In this study, we only used MDCK-SIAT1 cells, although both, MDCK-SIAT1 and hCK have successfully been used in FRA assays (Koszalka et al., 2020; Takashita et al., 2020a).

We demonstrated that, like HINT, IRINA can be used for antigenic analysis of HA using mAb or polyclonal antiserum. IRINA results using ferret antisera demonstrated that most of A(H3N2) viruses circulating in the US during the 2021–2022 season were antigenically different from cell-grown A/Cambodia/e0826360/2020, but similar to the 2022 southern hemisphere vaccine cell prototype virus A/Darwin/6/2021. These findings are in good agreement with HINT results submitted for the WHO vaccine composition consultation meeting held in February 2022 (https://cdn.who.int/media/docs/default-source/influenza/who-influenza-recommendations/vcm-northern-hemisphere-recommendation-2022-2023/202202_recommendation.pdf). Moreover, IRINA was able to detect a 3-4-fold reduced reactivity of antiserum raised against A/Darwin/6/2021 with viruses that had either an amino acid substitution at residue 222 or a combination of substitutions at 205 and 212 in the HA. It is worth noting that in certain instances, fold reduction in neutralization titers were 3–4 times lower for IRINA as compared to HINT (e.g., reactivity of anti-A/Cambodia/e0826360/2020 serum towards A/Darwin/6/2021 or A/Montana/01/2021) (Table 4). This difference likely stemmed from the inhibition of NA activity on infected cells (signal readout for IRINA) by anti-NA antibodies present in the serum. To this end, we observed that fold reduction in IRINA titers were very similar to HINT when supernatant was removed following attachment of cells at 2–3 hpi (Table S4). Therefore, when using IRINA to test convalescent sera, it would be prudent to remove residual antiserum shortly (~2–3 h) after infection.

In conclusion, IRINA offers advantages over current laboratory methods as it provides a unified platform to test susceptibility of influenza viruses to antivirals with different mechanisms of action. This is important as it will allow surveillance laboratories to obtain more data faster while requiring fewer investments and resources. Like HINT, IRINA can likely be used to assess susceptibility to RNA polymerase inhibitors (e.g., pimodivir) and other direct-acting antivirals (Patel et al., 2021). It may also be applied to testing anti-NA antibodies that target the NA active site and whose activity can be detected using a small substrate like MUNANA. Implementation of IRINA can streamline phenotypic characterization of emerging viruses and could prove vital to improve virological surveillance and pandemic preparedness.

Supplementary Material

Refer to Web version on PubMed Central for supplementary material.

Acknowledgements

We are thankful to the US public health laboratories and other laboratories participating in World Health Organization Global Influenza and Surveillance and Response System (WHO-GISRS) for productive collaboration with the CDC Influenza Division and their timely submission of influenza viruses. We are appreciative of the kind gift of MDCK-SIAT1 cells by Dr. M. Matrosovich. The authors would like to thank Dr. Emi Takashita from Tokyo WHO Collaborating Centre for Reference and Research on Influenza for kindly providing an A(H3N2) virus with primary baloxavir resistant substitution, PA-I38T and corresponding sequence matched control virus. The authors are most grateful to Shionogi and Co., LTD. for kindly providing baloxavir acid for phenotypic testing. We would like to acknowledge the valuable contributions of colleagues from the Virology, Surveillance and Diagnosis Branch of the CDC Influenza Division.

Funding source

This study was supported by the Influenza Division of Centers for Disease Control and Prevention (CDC).

Disclaimer

The finding and conclusions of this report are those of the authors and do not necessarily represent the views of the funding institution.

Data availability

Data will be made available on request.

References

Barman S, Adhikary L, Chakrabarti AK, Bernas C, Kawaoka Y, Nayak DP, 2004. Role of transmembrane domain and cytoplasmic tail amino acid sequences of influenza a virus neuraminidase in raft association and virus budding. J. Virol 78, 5258–5269. [PubMed: 15113907]

Corti D, Voss J, Gamblin SJ, Codoni G, Macagno A, Jarrossay D, Vachieri SG, Pinna D, Minola A, Vanzetta F, Silacci C, Fernandez-Rodriguez BM, Agatic G, Bianchi S, Giacchetto-Sasselli I, Calder L, Sallusto F, Collins P, Haire LF, Temperton N, Langedijk JP, Skehel JJ, Lanzavecchia A, 2011. A neutralizing antibody selected from plasma cells that binds to group 1 and group 2 influenza A hemagglutinins. Science 333, 850–856. [PubMed: 21798894]

Deyde VM, Xu X, Bright RA, Shaw M, Smith CB, Zhang Y, Shu Y, Gubareva LV, Cox NJ, Klimov AI, 2007. Surveillance of resistance to adamantanes among influenza A(H3N2) and A(H1N1) viruses isolated worldwide. J. Infect. Dis 196, 249–257. [PubMed: 17570112]

Eichelberger MC, Hassantoufighi A, Wu M, Li M, 2008. Neuraminidase activity provides a practical read-out for a high throughput influenza antiviral screening assay. Virol. J 5, 109. [PubMed: 18822145]

Govorkova EA, Takashita E, Daniels RS, Fujisaki S, Presser LD, Patel MC, Huang W, Lackenby A, Nguyen HT, Pereyaslov D, Rattigan A, Brown SK, Samaan M, Subbarao K, Wong S, Wang D, Webby RJ, Yen HL, Zhang W, Meijer A, Gubareva LV, 2022. Global update on the susceptibilities of human influenza viruses to neuraminidase inhibitors and the cap-dependent endonuclease inhibitor baloxavir, 2018-2020. Antivir. Res 200, 105281. [PubMed: 35292289]

Gross FL, Bai Y, Jefferson S, Holiday C, Levine MZ, 2017. Measuring Influenza Neutralizing Antibody Responses to A(H3N2) Viruses in Human Sera by Microneutralization Assays Using MDCK-SIAT1 Cells. J Vis Exp.

Gubareva LV, 2004. Molecular mechanisms of influenza virus resistance to neuraminidase inhibitors. Virus Res. 103, 199–203. [PubMed: 15163510]

Gubareva LV, Mishin VP, Patel MC, Chesnokov A, Nguyen HT, De La Cruz J, Spencer S, Campbell AP, Sinner M, Reid H, Garten R, Katz JM, Fry AM, Barnes J, Wentworth DE, 2019. Assessing baloxavir susceptibility of influenza viruses circulating in the United States during the 2016/17 and 2017/18 seasons. Euro Surveill. 24, 1800666. [PubMed: 30670144]

Hassantoufighi A, Zhang H, Sandbulte M, Gao J, Manischewitz J, King L, Golding H, Straight TM, Eichelberger MC, 2010. A practical influenza neutralization assay to simultaneously quantify hemagglutinin and neuraminidase-inhibiting antibody responses. Vaccine 28, 790–797. [PubMed: 19887135]

Hayden FG, Sugaya N, Hirotsu N, Lee N, de Jong MD, Hurt AC, Ishida T, Sekino H, Yamada K, Portsmouth S, Kawaguchi K, Shishido T, Arai M, Tsuchiya K, Uehara T, Watanabe A, Baloxavir Marboxil Investigators G, 2018. Baloxavir marboxil for uncomplicated influenza in adults and adolescents. N. Engl. J. Med 379, 913–923. [PubMed: 30184455]

Ince WL, Smith FB, O'Rear JJ, Thomson M, 2020. Treatment-emergent influenza virus PA substitutions independent of those at I38 associated with reduced baloxavir susceptibility and virus rebound in trials of baloxavir marboxil. J. Infect. Dis 222, 957–961. [PubMed: 32253432]

Jester B, Schwerzmann J, Mustaquim D, Aden T, Brammer L, Humes R, Shult P, Shahangian S, Gubareva L, Xu X, Miller J, Jernigan D, 2018. Mapping of the US domestic influenza virologic surveillance landscape. Emerg. Infect. Dis 24, 1300–1306. [PubMed: 29715078]

Jorquera PA, Mishin VP, Chesnokov A, Nguyen HT, Mann B, Garten R, Barnes J, Hodges E, De La Cruz J, Xu X, Katz J, Wentworth DE, Gubareva LV, 2019. Insights into the antigenic advancement of influenza A(H3N2) viruses, 2011-2018. Sci. Rep 9, 2676. [PubMed: 30804469]

Kallewaard NL, Corti D, Collins PJ, Neu U, McAuliffe JM, Benjamin E, Wachter-Rosati L, Palmer-Hill FJ, Yuan AQ, Walker PA, Vorlaender MK, Bianchi S, Guarino B, De Marco A, Vanzetta F, Agatic G, Foglierini M, Pinna D, Fernandez-Rodriguez B, Fruehwirth A, Silacci C, Ogrodowicz RW, Martin SR, Sallusto F, Suzich JA, Lanzavecchia A, Zhu Q, Gamblin SJ, Skehel JJ, 2016. Structure and function analysis of an antibody recognizing all influenza A subtypes. Cell 166, 596–608. [PubMed: 27453466]

Karakus U, Crameri M, Lanz C, Yángüez E, 2018. Propagation and titration of influenza viruses. Methods Mol. Biol 1836, 59–88. [PubMed: 30151569]

Koszalka P, Farrukee R, Mifsud E, Vijaykrishna D, Hurt AC, 2020. A rapid pyrosequencing assay for the molecular detection of influenza viruses with reduced baloxavir susceptibility due to PA/I38X amino acid substitutions. Influenza Other Respir Viruses 14, 460–464. [PubMed: 32045100]

Lin Y, Gu Y, Wharton SA, Whittaker L, Gregory V, Li X, Metin S, Cattle N, Daniels RS, Hay AJ, McCauley JW, 2015. Optimisation of a microneutralisation assay and its application in antigenic characterisation of influenza viruses. Influenza Other Respir Viruses 9, 331–340. [PubMed: 26073976]

Lin Y, Wharton SA, Whittaker L, Dai M, Ermetal B, Lo J, Pontoriero A, Baumeister E, Daniels RS, McCauley JW, 2017. The characteristics and antigenic properties of recently emerged subclade 3C.3a and 3C.2a human influenza A(H3N2) viruses passaged in MDCK cells. Influenza Other Respir Viruses 11, 263–274. [PubMed: 28164446]

Matrosovich M, Matrosovich T, Carr J, Roberts NA, Klenk HD, 2003. Overexpression of the alpha-2,6-sialyltransferase in MDCK cells increases influenza virus sensitivity to neuraminidase inhibitors. J. Virol 77, 8418–8425. [PubMed: 12857911]

Meijer A, Rebelo-de-Andrade H, Correia V, Besselaar T, Drager-Dayal R, Fry A, Gregory V, Gubareva L, Kageyama T, Lackenby A, Lo J, Odagiri T, Pereyaslov D, Siqueira MM, Takashita E, Tashiro M, Wang D, Wong S, Zhang W, Daniels RS, Hurt AC, 2014. Global update on the susceptibility of human influenza viruses to neuraminidase inhibitors, 2012-2013. Antivir. Res 110, 31–41. [PubMed: 25043638]

Mohan T, Nguyen HT, Kniss K, Mishin VP, Merced-Morales AA, Laplante J, St George K, Blevins P, Chesnokov A, De La Cruz JA, Kondor R, Wentworth DE, Gubareva LV, 2021. Cluster of oseltamivir-resistant and hemagglutinin antigenically drifted influenza A(H1N1)pdm09 viruses, Texas, USA, January 2020. Emerg. Infect. Dis 27, 1953–1957. [PubMed: 34152954]

Nayak DP, Reichl U, 2004. Neuraminidase activity assays for monitoring MDCK cell culture derived influenza virus. J. Virol. Methods 122, 9–15. [PubMed: 15488615]

Noshi T, Kitano M, Taniguchi K, Yamamoto A, Omoto S, Baba K, Hashimoto T, Ishida K, Kushima Y, Hattori K, Kawai M, Yoshida R, Kobayashi M, Yoshinaga T, Sato A, Okamatsu M, Sakoda Y, Kida H, Shishido T, Naito A, 2018. In vitro characterization of baloxavir acid, a first-in-class cap-dependent endonuclease inhibitor of the influenza virus polymerase PA subunit. Antivir. Res 160, 109–117. [PubMed: 30316915]

Okomo-Adhiambo M, Sleeman K, Lysén C, Nguyen HT, Xu X, Li Y, Klimov AI, Gubareva LV, 2013. Neuraminidase inhibitor susceptibility surveillance of influenza viruses circulating worldwide during the 2011 Southern Hemisphere season. Influenza Other Respir Viruses 7, 645–658. [PubMed: 23575174]

Omoto S, Speranzini V, Hashimoto T, Noshi T, Yamaguchi H, Kawai M, Kawaguchi K, Uehara T, Shishido T, Naito A, Cusack S, 2018. Characterization of influenza virus variants induced by treatment with the endonuclease inhibitor baloxavir marboxil. Sci. Rep 8, 9633. [PubMed: 29941893]

Patel MC, Chesnokov A, Jones J, Mishin VP, De La Cruz JA, Nguyen HT, Zanders N, Wentworth DE, Davis TD, Gubareva LV, 2021. Susceptibility of widely diverse influenza A viruses to PB2 polymerase inhibitor pimodivir. Antivir. Res 188, 105035. [PubMed: 33581212]

Ruppach H, 2013/2014. Log_{10} reduction factors in viral clearance studies. Bioprocess J 12. https://www.criver.com/sites/default/files/resources/Log10ReductionFactorsinViralClearanceStudies.pdf.

Takada K, Kawakami C, Fan S, Chiba S, Zhong G, Gu C, Shimizu K, Takasaki S, Sakai-Tagawa Y, Lopes TJS, Dutta J, Khan Z, Kriti D, van Bakel H, Yamada S, Watanabe T, Imai M, Kawaoka Y, 2019. A humanized MDCK cell line for the efficient isolation and propagation of human influenza viruses. Nature Microbiol. 4, 1268–1273. [PubMed: 31036910]

Takashita E, Abe T, Morita H, Nagata S, Fujisaki S, Miura H, Shirakura M, Kishida N, Nakamura K, Kuwahara T, Mitamura K, Ichikawa M, Yamazaki M, Watanabe S, Hasegawa H, Influenza Virus Surveillance Group of, J., 2020a. Influenza A(H1N1)pdm09 virus exhibiting reduced susceptibility to baloxavir due to a PA E23K substitution detected from a child without baloxavir treatment. Antivir. Res 180, 104828. [PubMed: 32574689]

Takashita E, Daniels RS, Fujisaki S, Gregory V, Gubareva LV, Huang W, Hurt AC, Lackenby A, Nguyen HT, Pereyaslov D, Roe M, Samaan M, Subbarao K, Tse H, Wang D, Yen HL, Zhang W, Meijer A, 2020b. Global update on the susceptibilities of human influenza viruses to neuraminidase inhibitors and the cap-dependent endonuclease inhibitor baloxavir, 2017-2018. Antivir. Res 175, 104718. [PubMed: 32004620]

Takashita E, Hiroko M, Ogawa R, Nakamura K, Fujisaki S, Shirakura M, Kuwahara T, Kishida N, Watanabe S, Odagiri T, 2018. Susceptibility of influenza viruses to the novel cap-dependent endonuclease inhibitor baloxavir marboxil. Front. Microbiol 9, 3026. [PubMed: 30574137]

Tisdale M, 2000. Monitoring of viral susceptibility: new challenges with the development of influenza NA inhibitors. Rev. Med. Virol 10, 45–55. [PubMed: 10654004]

van Baalen CA, Jeeninga RE, Penders GH, van Gent B, van Beek R, Koopmans MP, Rimmelzwaan GF, 2017. ViroSpot microneutralization assay for antigenic characterization of human influenza viruses. Vaccine 35, 46–52. [PubMed: 27899226]

WHO, 2012. Meetings of the WHO working group on surveillance of influenza antiviral susceptibility – Geneva. Wkly. Epidemiol. Rec 87, 369–374. November 2011 and June 2012. [PubMed: 23061103]

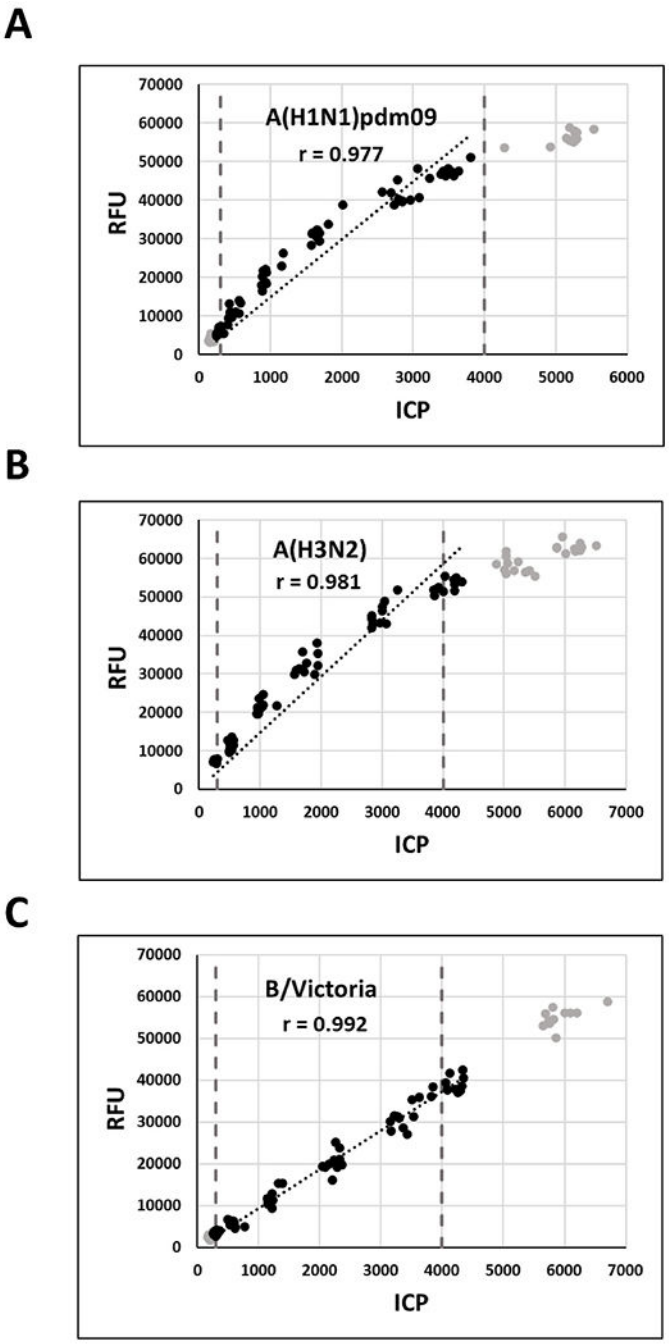

Fig. 1.

Linear relationship between infected cell population (ICP) and the NA activity of infected cells. Three viruses, A/Illinois/08/2018 (A), A/Louisiana/50/2017 (B), and B/North Carolina/25/2018 (C) representing A(H1N1)pdm09, A(H3N2), and B/Victoria lineage, respectively, were serially diluted to determine the relationship of ICP and NA activity (expressed in RFU) of infected cells. Plotted data is representative of three independent experiments. Dashed grey lines indicate cut-offs for acceptable ICP range. Black dots represent values used for best-fit trendline (black dotted line) with 95% confidence. The

correlation coefficients (r) between ICP and RFU were calculated by the Pearson correlation test (p = < 0.0001). RFU: relative fluorescence units.

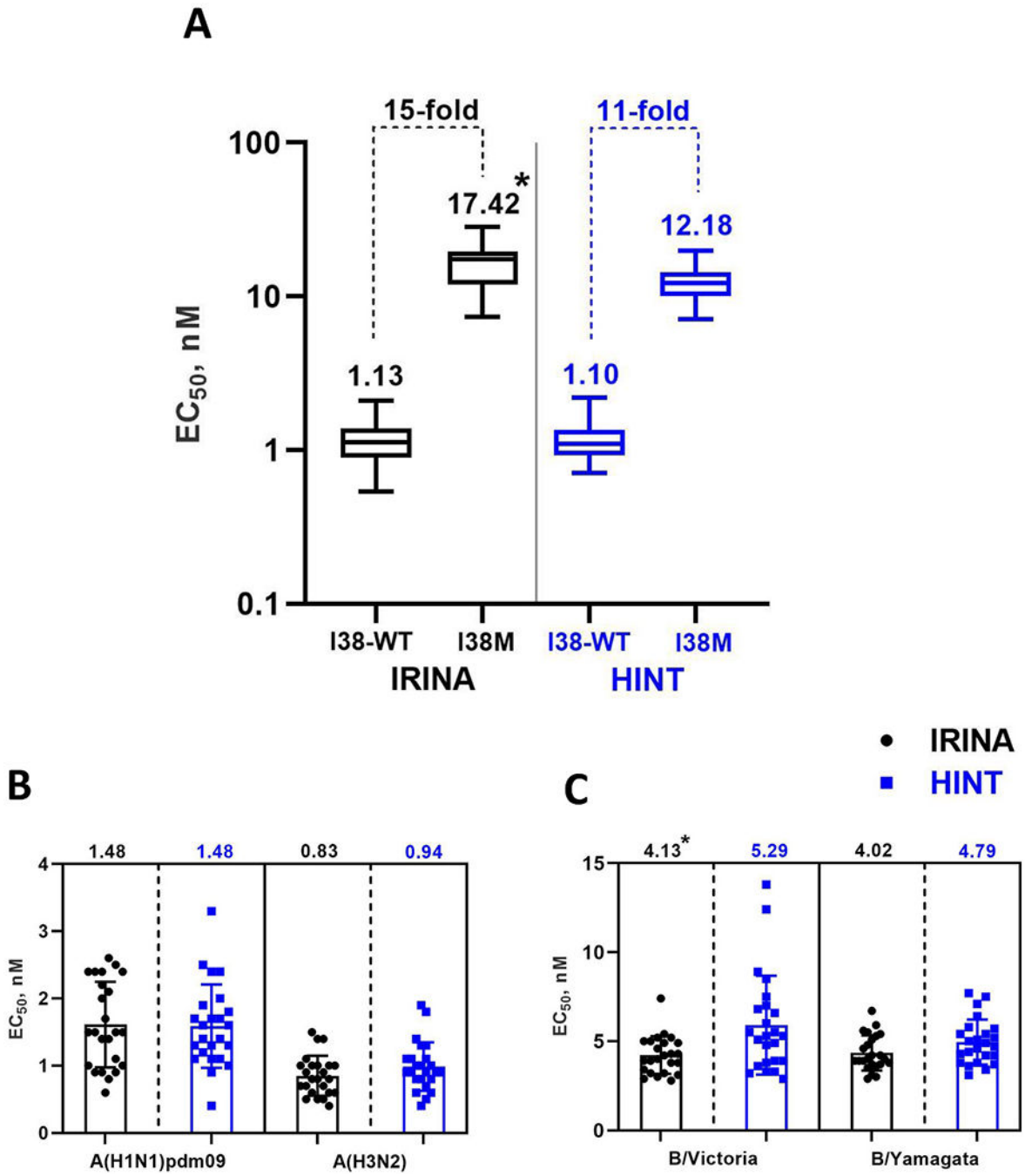

Fig. 2.

Baloxavir susceptibility testing of reference and surveillance viruses using IRINA and HINT. (A) Pair of A(H3N2) viruses (A/Louisiana/50/2017-PA-I38 and A/Louisiana/49/2017-PA-I38M) tested in a minimum of six independent experiments. Virus inoculum was determined by NA activity for IRINA, and ICP for HINT. EC_{50} values were calculated using RFU for IRINA, and ICP for HINT and shown as box and whiskers plots, where whiskers stretch to the minimum and maximum EC_{50} values. Median EC_{50} and corresponding fold increase values are indicated. (B, C) Results for surveillance viruses

(n = 96): A (H1N1)pdm09 and A(H3N2) subtypes (B), and B/Victoria and B/Yamagata lineages (C). IRINA and HINT were conducted separately, each in at least two independent experiments. Median EC_{50} values are indicated, and standard deviations are shown as error bars. (A–C) Unpaired student's t-test was used for statistical comparison of EC_{50} values determined using IRINA vs. HINT. * indicates statistically significant difference ($P < 0.05$).

Table 1

Infected cell population (ICP) and NA activity: reference viruses.

Virus name	Subtype or lineage	No. of experiments (total replicates)	Parameter	Range	Median	Average ± SD
A/Illinois/08/2018[a]	H1N1pdm09	14 (126)	ICP	706–1766	1152	1158 ± 210
			RFU	15388–43043	27230	27189 ± 5986
A/Louisiana/50/2017[a]	H3N2	14 (149)	ICP	715–1951	1037	1138 ± 314
			RFU	17741–42232	27287	28384 ± 6181
B/North Carolina/25/2018[b]	Victoria	8 (81)	ICP	894–2327	1189	1330 ± 364
			RFU	7913–32936	14842	15805 ± 6398

RFU: relative fluorescence unit; SD: standard deviation.

Target ICP is 1000. ICP and NA activity (expressed in RFU) were determined at 24 hpi.

[a]Viruses from CDC baloxavir susceptibility reference panel, v1.1 (IRR cat. #FR-1678).

[b]Virus from CDC neuraminidase inhibitor susceptibility reference virus panel, v3.0 (IRR cat. #FR-1755).

Table 2

Baloxavir EC_{50} and fold increase for viruses containing polymerase acidic (PA) amino acid substitutions using IRINA and HINT assays.

(Sub)type or lineage	Virus name	PA AA[a]	IRINA		HINT	
			EC_{50} nM Average ± SD	Fold increase	EC_{50} nM Average ± SD	Fold increase
A(H1N1)pdm09	A/Texas/121/2018	E23	0.97 ± 0.19		1.53 ± 0.54	
	A/Arizona/35/2018	E23G	3.36 ± 0.29	3	5.21 ± 1.54	3
	A/Bolivia/1810/2018	K34	0.86 ± 0.34		1.26 ± 0.39	
	A/West Virginia/02/2019	K34R	3.15 ± 0.65	4	5.15 ± 1.16	4
	A/Illinois/08/2018[b]	I38	1.35 ± 0.07		1.69 ± 0.38	
	A/Illinois/37/2018[b]	I38L	10.30 ± 3.13	8	16.34 ± 4.32	10
	A/Illinois/08/2018	I38S	102.00 ± 41.26	75	86.76 ± 3.64	51
	A/Illinois/08/2018[b]	I38T	85.82 ± 28.06	63	107.05 ± 28.00	63
	A/South Carolina/11/2019	E199	0.62 ± 0.10		0.61 ± 0.17	
	A/Massachusetts/06/2019	E199G	1.96 ± 0.26	3	2.27 ± 0.66	4
A(H3N2)	A/Mexico/2822/2019	L28	0.70 ± 0.07		1.00 ± 0.27	
	A/Peru/113154619/2019	L28P	0.65 ± 0.15	1	1.01 ± 0.16	1
	A/Congo/319/2018	K34	0.46 ± 0.06		0.77 ± 0.21	
	A/Congo/732/2018	K34R	2.37 ± 0.28	5	2.82 ± 0.66	4
	A/Bangladesh/3007/2017	I38	0.65 ± 0.10		1.21 ± 0.41	
	A/Bangladesh/3007/2017	I38T	49.04 ± 9.31	75	100.64 ± 43.09	83
	A/Yokohama/136/2018	I38	0.56 ± 0.11		0.68 ± 0.14	
	A/Yokohama/133/2018	I38T	50.03 ± 19.15	90	38.67 ± 5.03	57
	A/Ulaanbaatar/1381/2019	I38	0.49 ± 0.11		0.71 ± 0.13	
	A/Michigan/390/2019	I38L	2.26 ± 0.28	5	6.61 ± 2.67	9
	A/Hawaii/67/2016	I38	0.42 ± 0.08		0.59 ± 0.07	
	A/Hawaii/89/2016	I38V	0.86 ± 0.15	2	0.81 ± 0.34	1
B/Victoria	B/Nevada/12/2020	I38	2.96 ± 0.74		3.78 ± 0.75	
	B/Lebanon/12/2020	I38V	4.80 ± 0.68	2	5.64 ± 0.51	1
B/Yamagata	B/Texas/98/2017	I38	2.48 ± 0.38		2.19 ± 0.46	
	B/Oregon/07/2018	I38V	4.27 ± 0.58	2	5.36 ± 2.79	2

HINT: high content imaging-based neutralization test; IRINA: influenza replication inhibition neuraminidase-based assay; SD: standard deviation; AA: amino acid. At least three independent tests were conducted. Fold increase in EC_{50} compared to sequence-matched control virus.

[a] PA amino acid sequences of control virus(es) is identical to those of mutant virus(es) except for the indicated residue.

[b] Viruses from CDC baloxavir susceptibility reference panel, v1.1 (IRR cat. #FR-1678).

Table 3

IC_{50} and fold for viruses containing neuraminidase amino acid substitutions using IRINA and NI assays.

(Sub)type or lineage	Virus name	NA AA[a]	IC_{50} nM, Average ± SD (Fold)							
			Oseltamivir		Zanamivir		Peramivir		Laninamivir	
			IRINA	NI	IRINA	NI	IRINA	NI	IRINA	NI
A(H1N1)pdm09	A/ Wyoming/02/2019	I223	0.35 ± 0.15	0.27; 0.30	0.35 ± 0.09	0.23; 0.25	0.15 ± 0.05	0.07; 0.08	0.45 ± 0.14	0.21; 0.24
	A/ Argentina/264/2018	I223K	3.57 ± 0.92 (**10**)	4.39 ± 1.01 (**15**)	0.60 ± 0.29 (2)	0.78 ± 0.09 (3)	0.27 ± 0.03 (2)	0.19 ± 0.07 (2.5)	0.90 ± 0.18 (2)	0.61 ± 0.02 (3)
	A/Hawaii/70/2019	I223	0.43 ± 0.14	0.14; 0.20	0.35 ± 0.07	0.20; 0.18	0.15 ± 0.03	0.05; 0.08	0.39 ± 0.03	0.21; 0.23
	A/New York/16/2020	I223K	5.05 ± 1.41 (**12**)	3.25 ± 0.41 (**19**)	0.70 ± 0.09 (2)	0.67 ± 0.04 (4)	0.32 ± 0.12 (2)	0.23 ± 0.03 (3.5)	0.93 ± 0.08 (2)	0.80 ± 0.10 (4)
	A/ Tennessee/17/2018	I223	0.29 ± 0.06	0.25; 0.26	0.34 ± 0.03	0.24; 0.29	0.16 ± 0.02	0.09; 0.09	0.47 ± 0.03	0.24; 0.27
	A/Iowa/73/2018	I223M	9.08 ± 2.31 (**31**)	3.82 ± 1.00 (**15**)	0.91 ± 0.21 (3)	0.34 ± 0.06 (1)	0.27 ± 0.06 (2)	0.08 ± 0.02 (1)	0.53 ± 0.07 (1)	0.21 ± 0.02 (1)
	A/ California/18/2019	I223	0.53 ± 0.27	0.34; 0.36	0.38 ± 0.09	0.25; 0.27	0.16 ± 0.03	0.07; 0.08	0.43 ± 0.06	0.20; 0.22
	A/Santiago/ 108999/2018	I223L	3.30 ± 0.27 (6)	2.79 ± 0.77 (8)	0.26 ± 0.02 (1)	0.26 ± 0.04 (1)	0.15 ± 0.02 (1)	0.09 ± 0.02 (1)	0.34 ± 0.05 (1)	0.26 ± 0.03 (1)
	A/Illinois/45/2019[b]	H275	0.64 ± 0.21	0.14 ± 0.03	0.41 ± 0.10	0.18 ± 0.01	0.16 ± 0.04	0.07 ± 0.01	0.39 ± 0.07	0.22 ± 0.02
	A/ Alabama/03/2020[b]	H275Y	278.77 ± 73.60 (**436**)	154.44 ± 37.20 (**1103**)	0.43 ± 0.09 (1)	0.27 ± 0.04 (2)	24.74 ± 3.40 (**155**)	14.12 ± 2.56 (**202**)	0.69 ± 0.11 (2)	0.50 ± 0.07 (2)
	A/Maine/01/2021	N295	0.90 ± 0.14	0.46; 0.45	0.46 ± 0.01	0.26; 0.26	0.26 ± 0.02	0.10; 0.11	0.63 ± 0.05	0.27; 0.30
	A/West Virginia/09/2020	N295S	71.65 ± 7.00 (**80**)	41.78 ± 10.80 (**92**)	1.05 ± 0.27 (2)	0.67 ± 0.11 (3)	1.62 ± 0.62 (6)	1.12 ± 0.17 (**11**)	0.89 ± 0.11 (1)	0.94 ± 0.18 (3)
A(H3N2)	A/ Pennsylvania/46/2015[b]	E119	0.42 ± 0.11	0.14 ± 0.03	0.40 ± 0.10	0.22 ± 0.05	0.22 ± 0.05	0.07 ± 0.02	0.50 ± 0.06	0.28 ± 0.10
	A/ Washington/33/2014 *b*	E119V	63.92 ± 24.59 (**152**)	29.67 ± 9.12 (**212**)	0.64 ± 0.24 (2)	0.38 ± 0.08 (2)	0.23 ± 0.03 (1)	0.10 ± 0.03 (1)	0.52 ± 0.14 (1)	0.39 ± 0.10 (1)
	A/ Washington/01/2007	R292	0.10 ± 0.02	0.13 ± 0.01	1.20 ± 0.21	1.29 ± 00.21	0.14 ± 0.03	0.15 ± 0.03	0.71 ± 0.06	0.55 ± 0.09

(Sub)type or lineage	Virus name	NA AA[a]	IC50 nM, Average ± SD (Fold)							
			Oseltamivir		Zanamivir		Peramivir		Laninamivir	
			IRINA	NI	IRINA	NI	IRINA	NI	IRINA	NI
	A/ Bethesda/956/2006	R292K	>1000.00 (**>10000**)	>1000.00 (**>10000**)	10.51 ± 4.42 (9)	10.40; 10.27 (8)	18.42 ± 11.88 (**132**)	24.15; 24.58 (**162**)	3.21 ± 0.79 (4.5)	3.71; 4.17 (7)
B/Victoria	B/Laos/0080/2016[b]	H134	22.76 ± 7.83	11.57 ± 2.60	3.36 ± 0.60	1.21 ± 0.42	1.00 ± 0.33	0.36 ± 0.07	2.03 ± 0.24	1.16 ± 0.30
	B/Laos/0654/2016[b]	H134N	70.85 ± 17.30 (3)	41.88 ± 6.93 (4)	274.65 ± 26.95 (**82**)	130.19 ± 24.87 (**108**)	67.81 ± 18.49 (**68**)	36.66 ± 6.91 (**102**)	124.76 ± 34.63 (**61.5**)	66.96 ± 20.67 (**58**)
	B/Memphis/20/96	R150	5.95 ± 2.71	7.92; 10.38	1.33 ± 0.15	1.45; 1.51	0.50 ± 0.07	0.54; 0.42	1.86 ± 0.23	1.37; 1.65
	B/Memphis/20/96	R150K	>1000 (**>168**)	>1000.00; 849.52 (**>120**)	92.56 ± 11.39 (**70**)	76,01; 87.09 (**55**)	342.05 ± 14.60 (**684**)	394.08; 347.04 (**772**)	291.39 ± 39.56 (**157**)	273.48; 310.43 (**193**)
	B/North Carolina/25/2018[b]	D197	25.75 ± 15.78	18.57 ± 7.12	2.84 ± 0.62	1.25 ± 0.47	0.98 ± 0.24	0.47 ± 0.22	2.04 ± 0.63	1,23 ± 0.36
	B/ Missouri/12/2018[b]	D197E	170.33 ± 76.84 (**7**)	155.68 ± 65.24 (**8**)	16.93 ± 4.76 (6)	10.81 ± 4.22 (**9**)	9.28 ± 3.68 (**9.5**)	10.56 ± 3.43 (**22.5**)	10.37 ± 3.00 (**5**)	3.69 ± 1.77 (3)
	B/South Carolina/02/2020	G243	15.22 ± 5.06	19.24; 19.48	2.21 ± 0.45	2.09; 2.23	0.77 ± 0.13	0.60; 0.63	1.94 ± 0.20	2.31; 2.31
	B/New Jersey/02/2020	G243S	492.29 ± 106.91 (**32**)	221.19 ± 51.22 (**11**)	38.88 ± 8.84 (**18**)	27.21 ± 9.43 (**13**)	38.15 ± 9.08 (**49.5**)	31.28 ± 8.08 (**51**)	5.35 ± 0.40 (3)	4.79 ± 0.73 (2)

AA: amino acid; IRINA: influenza replication inhibition neuraminidase-based assay; NI: neuraminidase inhibition assay; SD: standard deviation

Average ± SD of IC_{50}s are calculated from at least three independent tests. When virus was tested in less than three independent test, IC_{50} values from two independent tests are shown. Fold increase in IC_{50} compared to control virus. Values shaded in light grey indicate “reduced inhibition (RI)” (type A viruses 10-100-fold; type B viruses 5-50-fold), and dark grey indicate “highly reduced inhibition (HRI)” (type A viruses >100-fold; type B viruses >50-fold).

[a]Amino acid numbering is based on the NA (sub)type specific for type A viruses and the NA of type B viruses. NA amino acid sequences of control virus(es) is identical to those of mutant virus(es), except for the indicated residue. For each pair, wildtype control virus is listed first followed by the respective mutant virus. IC_{50} of respective wildtype virus is used to calculate fold increase in IC_{50} for corresponding NA mutant virus.

[b]Viruses from the CDC neuraminidase inhibitor susceptibility reference virus panel, v3.0 (IRR cat. #FR-1755).

Table 4

Antigenic analysis of influenza A(H3N2) viruses, United States, 2021–2022.

Virus	HA1 amino acid changes compared to A/Darwin/6/2021[a]	Ferret antisera			
		IRINA titers, Average ± SD (fold)		HINT titers, Average ± SD (fold)	
		Cam/e0826360/20	Darwin6/21	Cam/e0826360/20	Darwin6/21
Reference					
A/Cambodia/e0826360/2020	G53D, S156H, N159Y, I160T, Q164L, K171N, D186S, N190D, S198P	*3600 ± 855 (1.0)*	386 ± 113 (26.4)	*3428 ± 800 (1.0)*	126 ± 43 (84.3)
A/Darwin/6/2021		380 ± 109 (9.5)	*10181 ± 1474 (1.0)*	<80 (>43)	*10581 ± 3148 (1.0)*
Test					
A/Montana/01/2021		292 ± 126 (12.3)	17101 ± 5998 (0.6)	94 ± 22 (36.5)	19841 ± 7052 (0.5)
A/Arizona/03/2021	D104G, L157I, S262N, K276R	631 ± 133 (5.7)	18023 ± 5027 (0.6)	353 ± 205 (9.7)	15335 ± 4395 (0.7)
A/Maryland/05/2021	D104G, L157I, S262N, K276R	732 ± 421 (4.9)	14954 ± 4041 (0.7)	172 ± 44 (19.9)	17237 ± 4216 (0.6)
A/Massachusetts/03/2021	D104G, L157I, S262N, K276R	646 ± 171 (5.6)	15328 ± 2759 (0.7)	180 ± 79 (19)	14655 ± 3802 (0.7)
A/Tennessee/01/2021	D104G, L157I, S262N, K276R	477 ± 88 (7.6)	14596 ± 2774 (0.7)	176 ± 97 (19.4)	14198 ± 3435 (0.7)
A/Arizona/02/2021	I25V, G53N, N96S, I192F	548 ± 222 (6.6)	18762 ± 3796 (0.5)	187 ± 35 (18.3)	18686 ± 4029 (0.6)
A/District of Columbia/01/2021	I25V, G53N, N96S, I192F	403 ± 84 (8.9)	17683 ± 4687 (0.6)	207 ± 74 (16.6)	16548 ± 4228 (0.6)
A/Florida/02/2021	I25V, G53N, N96S, I192F	492 ± 173 (7.3)	18830 ± 5636 (0.5)	221 ± 35 (15.5)	19248 ± 5506 (0.5)
A/California/05/2021	I25V, G53N, N96S, I192F, R201S	395 ± 118 (9.1)	18786 ± 2170 (0.5)	191 ± 46 (17.9)	18881 ± 4274 (0.6)
A/Michigan/04/2021	E50K, G53D, S156H	234 ± 70 (15.4)	9069 ± 1822 (1.1)	203 ± 72 (16.9)	10549 ± 2713 (1.0)
A/Michigan/05/2021	E50K, G53D, S156H	192 ± 55 (18.8)	7038 ± 1728 (1.4)	193 ± 53 (17.7)	8974 ± 2286 (12)
A/Michigan/10/2021	E50K, G53D, S156H, R222K	159 ± 52 (22.7)	2825 ± 721 (3.6)	142 ± 42 (24.2)	3267 ± 1003 (3.2)
A/Florida/01/2022	G53D, S156H, S205F, A212T	566 ± 109 (6.4)	3197 ± 575 (3.2)	320 ± 90 (10.7)	3059 ± 759 (3.5)
A/Arizona/03/2022	G53D, S156H, S205F, A212T, S312S	602 ± 209 (6.0)	3029 ± 480 (3.4)	327 ± 76 (10.5)	2798 ± 640 (3.8)
A/Arizona/04/2022	G53D, S156H, S205F, A212T, S312S	470 ± 81 (7.7)	2511 ± 351 (4.1)	262 ± 55 (13.1)	2240 ± 484 (4.7)
A/Arizona/07/2022	G53D, S156H, S205F, A212T, S312S	509 ± 106 (7.1)	2872 ± 672 (3.5)	305 ± 81 (11.2)	2685 ± 766 (3.9)
A/New York/02/2021	G53D, H56Y, S156H, S205F, A212T, S270T	552 ± 142 (6.5)	3505 ± 830 (2.9)	326 ± 67 (10.5)	3220 ± 860 (3.3)
A/Pennsylvania/01/2021	N6D, G53D, S156H, S205F, A212T, R299K	706 ± 250 (5.1)	3182 ± 718 (3.2)	375 ± 147 (9.1)	2564 ± 714 (4.1)

HA: hemagglutinin; HINT: high content imaging-based neutralization test; IRINA: influenza replication inhibition neuraminidase-based assay; SD: standard deviation. Antigenic analysis of cell-propagated influenza A(H3N2) viruses, representing HA genetic clade 3C.2a1b.2a.2, was performed by IRINA and HINT using post-infection ferret antisera generated for two influenza A(H3N2) vaccine reference viruses: A/Cambodia/e0826360/2020 (Cam/e0826360/20) from 3C.2a1b.2a.1 was selected for the 2021–2022 northern hemisphere season, and A/Darwin/6/2021 (Darwin6/21) from 3C.2a1b.2a.2 was selected as a cell-based vaccine component for the 2022 southern hemisphere and 2022–2023 northern hemisphere seasons. The neutralization titer is the reciprocal dilution of antiserum needed to reduce the RFU or ICP by 50%.

Underlined italics indicate homologous titers. Number in parentheses indicate fold changes in titer compared to the respective homologous titers.

[a] Consensus amino acids in A/Darwin/6/2021 are: N6, I25, E50, G53, H56, N96, D104, S156, L157, N159, I160, Q164, K171, D186, N190, I192, S198, R201, S205, A212, R222, S262, S270, K276, R299, S312.